ELSEVIER

Thermochimica Acta 325 (1999) 157–165

thermochimica acta

Thermal dehydration of cobalt and zinc formate dihydrates by controlled-rate thermogravimetry (CRTG) and simultaneous X-ray diffractometry–differential scanning calorimetry (XRD-DSC)

Tadashi Arii*, Akira Kishi

Thermal Analysis Division, RIGAKU Corporation, 3-9-12 Matubara, Akishima, Tokyo 196-8666, Japan

Received 30 July 1998; received in revised form 5 October 1998; accepted 12 October 1998

Abstract

The thermal dehydration study of the similar hydrated salts, cobalt and zinc formate dihydrates, have been carried out successfully by means of X-ray diffractometry–differential scanning calorimetry (XRD-DSC) and controlled-rate thermogravimetry (CRTG). X-ray diffraction analysis recorded simultaneously indicates that the resulting anhydrous product, $Zn(HCO_2)_2$, was crystalline, while $Co(HCO_2)_2$ was amorphous.

The XRD-DSC data are proven to be invaluable in verifying the interpretation of overlapping processes in thermal events. In addition, these differences in the resulting anhydrous products can be explained from kinetic analysis results based on the CRTG data. The kinetic mechanism governing the dehydration of zinc formate dihydrate is a nucleation and growth process, while in the case of cobalt formate dihydrate a phase boundary controlled reaction is the governing mechanism.

Keywords: XRD-DSC; Kinetics; Controlled-rate thermogravimetry; Thermal dehydration; Recrystallization

1. Introduction

Generally speaking, thermal dehydration of hydrates is a reversible reaction and is influenced by the product phase, because such a residual material, more or less, tends to diminish the rate of the water diffusion from the reaction interface. It has been also known that the rate of thermal dehydration of hydrate is greatly affected by the experimental conditions, such as the sample size, the nature of the atmosphere, the crucible shape and the heating rate.

On the other hand, no single mechanistic explanation has been accepted as possessing general validity and several mechanistic models have been proposed as follows [1]: (1) properties of adsorbed water [2,3], (2) recrystallization of product phase [4], and (3) heat and gas transfer at the reaction and interface [5,6]. It may be possible that complex behaviors are concurrently caused by the above phenomena and different mechanisms may concurrently operate in different sample particles.

Phase transitions among the various solid states during solid reactions have been the focus of much attention for several decades, and a variety of methods have been used to study their thermodynamic, structural, and kinetic properties. Historically, differential

*Corresponding author. Fax: +81-42-544-9650; e-mail: t-arii@rigaku.co.jp

0040-6031/99/$ – see front matter
PII: S0040-6031(98)00574-7

scanning calorimetry (DSC) and X-ray diffractometry (XRD) have been utilized as the most powerful techniques.

In particular, DSC is widely accepted as a useful thermo-analytical tool for the study of phase transitions. However, for calorimetoric study, their thermal events may severely overlap, disturbing accurate calorimetric interpretation of the data in some cases. In addition to this, unfortunately, there are several types of thermal events which may not be related to structural transformations. Volatilization of guest molecules from inclusion compounds is one example [7]. Identification of each peak is often quite impossible without the aid of other analytical techniques, such as evolved-gas analysis and XRD, that yield information about structures and reactions.

One way to overcome this problem is to utilize both, temperature scanning X-ray diffraction and the calorimetric techniques. However, when comparing data obtained separately from both the methods, problems usually arise concerning the sampling methods, the experimental conditions and the instrumental differences, in particular with respect to temperature distribution in the sample environment under heating. These differences in measuring conditions complicate comparisons of the obtained data. Such problems can be overcome, however, by performing DSC and XRD measurements simultaneously on the same sample.

The development of the simultaneous measuring instrument of DSC and XRD has been anticipated for a few decades. In a previous report [8], we described the development of a new instrument which combines XRD capabilities with simultaneous thermal analysis, using power compensation differential scanning calorimetry (pc-DSC). During recent years, performances such as the accurate temperature measurement, sensitivity, resolution, and data handling have been substantially improved for both, the DSC and XRD.

From the viewpoint as methodology, controlled-rate thermal analysis (CRTA) [9–12] has become popular for these ten years. A constant reaction rate or a constant pressure of the evolved species in the reaction environment can be easily achieved at present. In our previous papers, we demonstrated that controlled-rate thermogravimetry (CRTG) represents a new approach for thermal methods offering significant advantages over conventional ones [13–16]. It especially leads us to an improved sensitivity and resolution in the thermogravimetry (TG) curves [17–20], and provides better kinetic data [21].

Although numerous studies have been performed on dehydration of organic and inorganic solids using TG, differential thermal analysis (DTA), DSC, XRD and other methods, the dehydration reaction is still one of the most complicated reactions. From the viewpoint of pure chemistry and industrial application, more detailed information as to the dehydration behavior of various solids and more versatile measuring instruments have been required for this purpose.

Masuda et al. [22,23] studied crystallinities of the dehydrated product phases and described the effect of water-vapor pressure on the kinetics of the thermal dehydration of some formate hydrates by means of a combination of TG-DTA and XRD. Their results reveal a few critical parameters in governing dehydration mechanism, these being the availability of atmospheric water molecules to form crystalline metal formates, the critical water-vapor pressures and the critical temperatures. These results imply that more sophisticated simultaneous instruments, under identical measuring conditions, are preferred to determine reaction mechanisms based on both, the structural and thermal data.

Our focus is on the interpretation of the actual dehydration mechanism of hydrated salts. In this paper, we analyze the complicated dehydration behavior of zinc and cobalt formate dihydrates measured by the XRD-DSC, in parallel with the results obtained by means of CRTG. Thereafter, we demonstrate the effectiveness for performing both the techniques of XRD-DSC and CRTG on these substances. Finally, we postulate that the kinetic mechanism of zinc salt dehydration is different from that of cobalt salt dehydration.

2. Experimental

2.1. Sample description

Commercially available zinc formate dihydrate ($Zn(OCH_2)_2 \cdot 2H_2O$) and cobalt formate dihydrate ($Co(OCH_2)_2 \cdot 2H_2O$) were recrystallized and kindly supplied by Masuda, and these was pulverized with a mortar and pestle, and sieved to a fraction below 150

mesh size. Each sample of about 30 mg in an open aluminum pan was used for the XRD-DSC and the CRTG measurements in static air.

2.2. Apparatus

An XRD-DSC apparatus was used and the instrumentation has been described in detail elsewhere [3]. The CRTG apparatus was Rigaku Thermo Plus TG-DTA 8120D thermogravimetry–differential thermal analyzer upgraded with a dynamic TG-DTA module, and a similar apparatus described in more detail elsewhere [19–21]. A sequence of experiments were carried out with a fully automated and computerized controlled-rate thermogravimetric analyzer (CRTG), and the rate of the mass loss is kept at a constant value ranging from 0.01 to 0.1% min^{-1}. In the CRTG experiments, a sample is heated at first at a constant heating rate such as 5 K min^{-1}, then at a proper switchover temperature the automatic control of the heating rate starts so that the rate of the mass loss is kept at a desired constant value. This measuring method is called the constant decomposition rate control, CDRC.

From a preliminary TG-DTA measurement at a constant heating rate, the proper switchover temperature was determined from the onset dehydration temperature. In the case of zinc formate dihydrate, here, the switchover temperature was set at 353 K and the rate of the mass loss over 353 K was kept at 0.06% min^{-1}, while that of cobalt formate dihydrate was 375 K. When the dehydration reaction is close to the end, the temperature increases markedly and the thermal run terminates.

3. Results

3.1. XRD-DSC analysis

The relationship between the DSC curve and X-ray diffraction profiles recorded during the dehydration of cobalt formate dihydrate by the simultaneous XRD-DSC is shown in Fig. 1 for a heating rate of 1 K min^{-1}. The DSC curve indicates that an initial dehydration begins at around 400 K and ends at around 445 K. This curve shows a broad endothermic peak, followed by a large and sharp endothermic peak

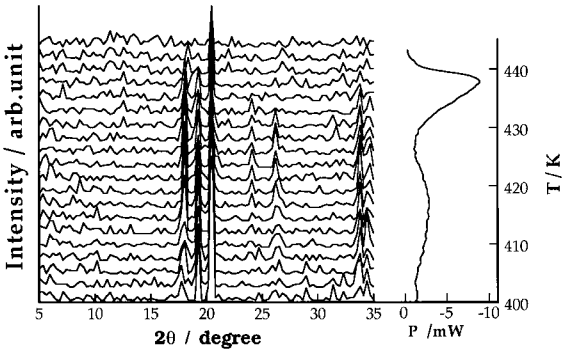

Fig. 1. Relationship between DSC curve and XRD patterns in the dehydration of $Co(HCO_2)_2 \cdot 2H_2O$ by simultaneous XRD-DSC.

with a maximum at 438 K. We can see that the intensity of XRD patterns changes dramatically and completely around the second endothermic peak maximum. After dehydration, the resulting product shows almost amorphous patterns. Fig. 2 shows the DSC curve and XRD patterns obtained at 380 and 440 K. Here, what is important is that the anhydrous product formed after the dehydration does not show crystalline patterns.

Similar results were obtained for the zinc formate dihydrate, and they have been already described elsewhere [8]. Fig. 3 shows the relationship between the DSC curve and X-ray diffraction patterns during the dehydration of zinc formate dihydrate, recorded by the simultaneous XRD-DSC. From the results, we can see that there is a large difference between the two salts in the decomposition temperature range as well as in the shape of DSC curve. Another difference is that the crystalline patterns are observed even after the dehydration of the zinc salt. This will lead us into a more detailed investigation.

Next, we performed the more detailed analysis of the dehydration behavior of cobalt formate dihydrate. The XRD total intensity curve is obtained by integration of intensity in the diffraction angle from 5° to 35°, and it is compared with the DSC curve in Fig. 4 as a function of temperature. It is evident from a decay of this total XRD intensity curve that the cobalt formate dihydrate is dehydrated slowly without any crystalline anhydrous product formation. A broad endothermic DSC peak and a slight increment of XRD intensity, observed from 400 to 425 K, would reflect some slight structural change of cobalt formate dihydrate.

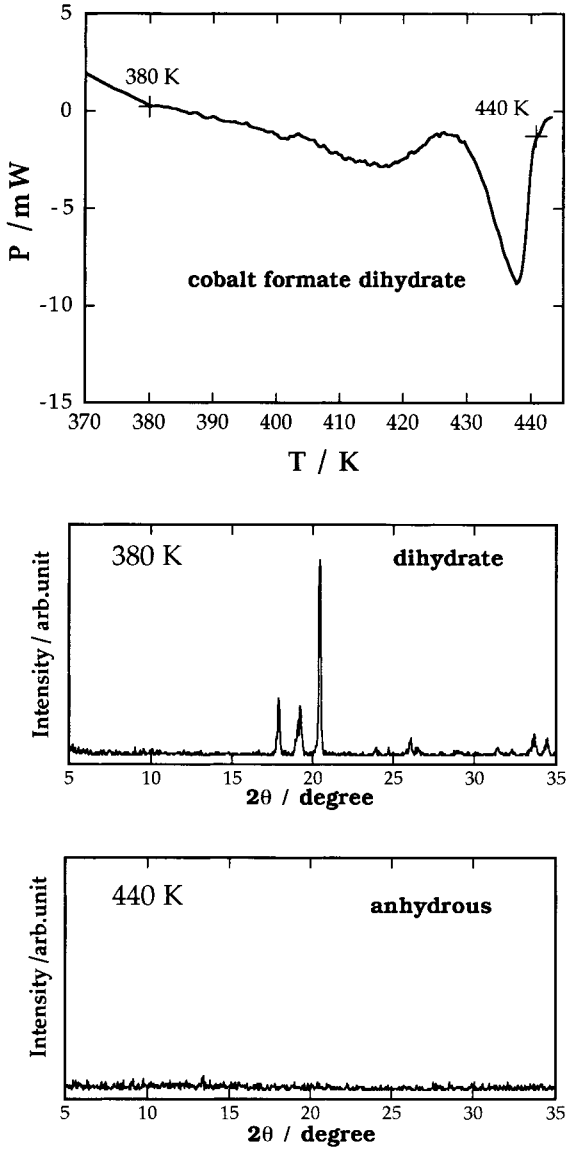

Fig. 2. DSC curve and XRD patterns obtained at 380 and 440 K in the dehydration of $Co(HCO_2)_2{\cdot}2H_2O$.

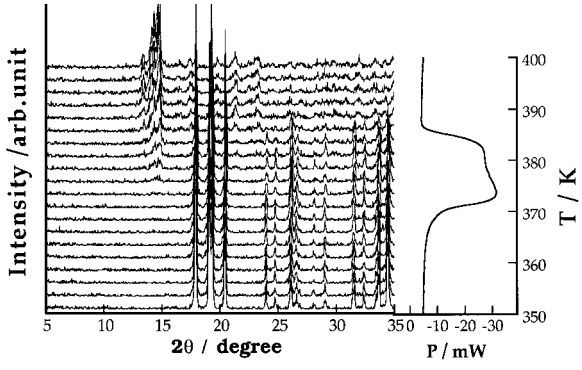

Fig. 3. Relationship between DSC curve and XRD patterns in the dehydration of $Zn(HCO_2)_2{\cdot}2H_2O$ by simultaneous XRD-DSC.

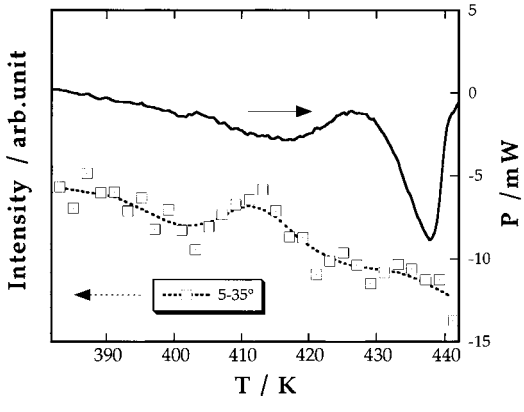

Fig. 4. Comparison of the DSC curve and the total integrated XRD curve obtained from the experimental diffraction angles in the dehydration of $Co(HCO_2)_2{\cdot}2H_2O$.

3.2. CRTG analysis

Our next interest is the relationship between the difference of dehydration mechanisms of both, the zinc and cobalt formate dihydrate XRD-DSC patterns. As described in our previous papers [21,24,25], the CRTG method offers significant advantages for the kinetic study of thermal decomposition over the conventional constant rate heating TG, because this method can easily offer the ability of constant reaction rate control, and assure small temperature and pressure gradients within a sample bed. We assume that the difference in the dehydration mechanisms of both the dihydrates can also be explained by the mass loss profiles obtained by the CRTG technique.

Fig. 5 shows TG-DTA curves of the dehydration of zinc and cobalt formate dihydrates obtained by the conventional heating rate method at 10 K min^{-1}. The dehydration of cobalt formate dihydrate proceeds gradually in the wide temperature range, from 360 to 460 K, while that of zinc formate dihydrate proceeds in a relatively narrow temperature range below 410 K. These data mean that the dehydration rate of zinc formate dihydrate is faster than that of cobalt salt

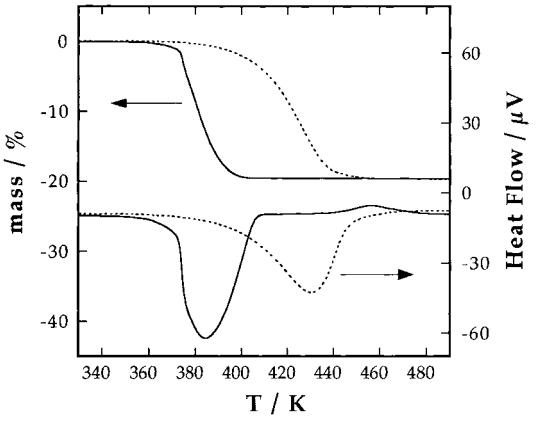

Fig. 5. TG-DTA curves for the dehydration of $Zn(HCO_2)_2{\cdot}2H_2O$ (———) and $Co(HCO_2)_2{\cdot}2H_2O$ (- - -) at a heating rate of 10 K min^{-1}.

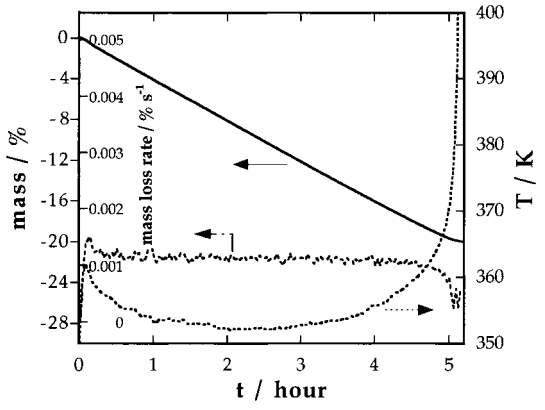

Fig. 6. Experimental CDRC curves under a reaction rate of 0.06% min^{-1} for the dehydration of $Zn(HCO_2)_2{\cdot}2H_2O$. Mass loss (———), temperature (· · ·) and derivative mass loss (- - -).

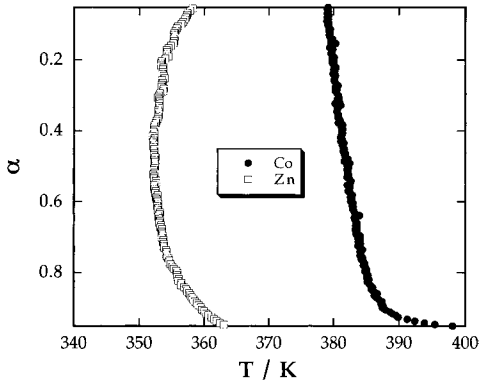

Fig. 7. Comparison of α vs. T in the dehydration processes of $Zn(HCO_2)_2{\cdot}2H_2O$ and $Co(HCO_2)_2{\cdot}2H_2O$ obtained by CDRC experiments.

and that such phenomena may be related to the crystallinities of both the dehydrated products. These profiles, however, would not indicate further important differences in the dehydration behavior of both the hydrated salts.

On the other hand, the CRTG measurement of zinc formate dihydrate gives a characteristic curve representing the nature of the dehydration process as shown in Fig. 6. Here, the temperature is automatically controlled so that the dehydration rate is maintained at a constant value of 0.06% min^{-1} according to the above-mentioned manner. The most important outcome of these data is the time vs. temperature profile. After the switchover temperature of 353 K, the temperature slightly increases at first, then gradually decreases as the constant rate dehydration begins. In the latter half of the dehydration reaction, the temperature gradually increases through a temperature minimum and then a marked temperature rise is observed, which is close to the end of the dehydration reaction.

Fig. 7 illustrates the comparison of the mass loss profiles during the dehydration of both the dihydrates obtained by the CRTG as a function of temperature. In this figure, α represents the fraction dehydrated. Here, we can see that unlike zinc formate dihydrate, cobalt formate dihydrate shows a gradual temperature rise from the very beginning of the dehydration reaction. We believe these characteristic profiles directly reflect the difference in dehydration mechanisms of both the dihydrates, and the kinetic analysis method based on these profiles will lead us to an elucidation of the most probable dehydration mechanisms as describe below.

3.3. Kinetic analysis of CRTG data

Before we describe our results, we shall discuss the theoretical background of solid-state reactions [26,27]. Preferential chemical reactions occurring at solid–solid interfaces are an essential feature of many solid-state reactions.

As a dehydration reaction proceeds, this interface progressively advances into unchanged reactants, and thereby the amount of reaction product increases. This

reaction usually yields microcrystals with cracks that provide escape path for the evolved water.

It is a general consensus that chemical change occurs almost exclusively within the interfacial zone, possibly as a consequence of strain at the plane of contact between the reactant and product phases. Systematic accounts of the derivation of the rate equations have found application in the solid-state decompositions. Integration of the rate expression incorporating both, the nucleation and growth terms given by Avrami–Erofeev have found wide application in kinetic analysis of the decomposition of solids. On the other hand, if initial nucleation is rapid and dense across all crystal faces and if those coalesce active interface are generated just beneath the original reactant surfaces, subsequent advance of this interface generates the geometry of volume contraction and the overall reaction will be effectively deceleratory.

We shall assume that the isothermal conversion rate, $d\alpha/dt$, is a linear function of a single temperature-dependent rate constant, k, and a temperature-independent function of the conversion, α, i.e.

$$d\alpha/dt = kf(\alpha) \tag{1}$$

and

$$k = A\exp(-E/RT) \tag{2}$$

where α is a fraction of the decomposed hydrate, $f(\alpha)$ a function depending on the kinetic model, A the pre-exponential factor, E the apparent activation energy, R the gas constant and T the absolute temperature. For $f(\alpha)$, normally, several assumed basic functions, derived from simply idealized models, are used for the kinetic study of the solid-state reactions, such as boundary controlled reactions, random nucleation and growth of nuclei or diffusion controlled reactions.

A combination of Eqs. (1) and (2) gives:

$$d\alpha/dt = A\exp(-E/RT)f(\alpha) \tag{3}$$

and, after taking logarithms, in the form:

$$\ln(d\alpha/dt/f(\alpha)) = \ln(A) - E/RT \tag{4}$$

In the Sharp method [28], $\ln(d\alpha/dt/f(\alpha))$ is plotted against the reciprocal absolute temperature $1/T$ for several assumed basic functions of $f(\alpha)$ which were derived from the idealized models. If the assumed $f(\alpha)$ is correct, a straight line is obtained, and the slope of this straight line and the intercept of its ordinate provide the activation energy E and the pre-exponential factor A, respectively.

When using the CDRC mode of the CRTG, the conversion rate, $d\alpha/dt$ at a constant value, C, then Eq. (4) becomes:

$$\ln(f(\alpha)) = -\ln(A/C) + E/RT \tag{5}$$

In view of the fact that the term ln (A/C) is a constant, plots of ln ($f(\alpha)$) against $1/T$ for various functions $f(\alpha)$ are theoretically sufficient to provide the kinetic parameters and the activation energy from a single CRTG experiment.

In addition, it follows that the general shape of the experimental curve of α against T, obtained under the condition of a constant reaction rate, is in itself quite significant for the elucidation of the actual reaction mechanism. This is demonstrated in Fig. 8, which shows the theoretical curves calculated by assuming the kinetic models [28] the following kinetic parameters: E=167 kJ mol^{-1}, A=2.0×10^{9} min^{-1} and C=3.0×10^{-2} min^{-1}. As clearly seen in Fig. 8, these curves are characteristic of the reaction mechanism. When such simple simulated results are shown graphically based on the available data, the relation is seen most clearly and the set of theoretical curves may be easily distinguished into three categories. In particular, the kinetic models of nucleation and growth given by Avrami–Erofeev lead to the profiles with a temperature minimum, which are not obtained either by linear raising temperature or isothermal measurements. The comparison of the α against T curve, obtained by a CRTG experiment with master curves based on various reaction models, is a fairly efficient means to determine the reaction mechanism.

4. Discussion

It has been recognized that the thermal dehydration of hydrated salts is still one of the most complicated reactions since the reaction is greatly influenced by the water-vapor pressure in the reaction atmosphere environment, including the self-generated atmosphere. Therefore, the presence of water molecules in the sample environment seems to directly influence the dehydration rate and crystallinities of the dehydrated product [22]. From the above-mentioned, a combination of data separately obtained by different, parallel

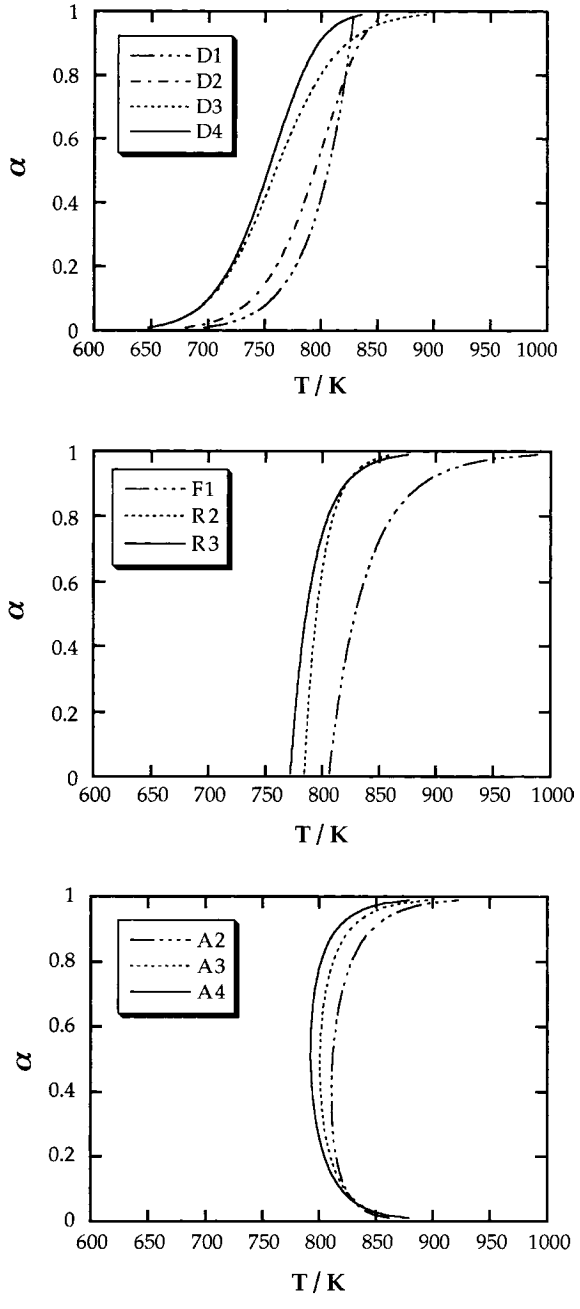

Fig. 8. Shape of the theoretical CRTA curves corresponding to the kinetic models assuming E=167 kJ mol^{-1}, A=2.0×10^{9} min^{-1} and C=3.0×10^{-2} min^{-1}.

apparatuses and specimens in the collecting structural and thermal data is often problematic, because the thermal dehydration of hydrated salts is affected markedly on the sample preparation and on the experimental conditions such as the sample size, the crucible shape and the heating rate, caused by instrumental limitation. To sum up, it must be borne in mind that any difference in measuring conditions complicates the combination and comparison of the obtained data, and then may lead us to an erroneous interpretation. This is a real limit to elucidating the thermal dehydration of hydrated salts. Consequently, the XRD-DSC is an especially powerful method for collecting structural and thermal data on such dehydration reaction where the integrated systematic measurement under identical conditions must be extremely important.

In the conventional linear heating rate methods, on the other hand, the dehydration of both salts indicates the mass losses with a monotonous decay, since the sample temperature follows the predetermined heating program as a function of time. These TG curves, however, would not directly indicate further significant differences between the dehydration behaviors, except for a difference of the approximate dehydration temperatures. Also, the linear heating rate method results in special problems of pressure, temperature gradients and porous structure of the solid products within the sample bed, because these unknown gradients cannot be specified in this method. This is also an actual obstruction in our understanding of the kinetic reaction. With the application of the CRTG method, uniform conditions exist throughout the sample and the sample environment by means of an appropriate control of the dehydration rate. In this respect, it is a desirable method for elucidating kinetic reaction mechanisms. In addition, the structural changes observed by the XRD-DSC give the strongest proof for an explanation of the actual mass loss curves during the dehydration obtained from the CRTG.

The profile of the experimental CDRC curve in the dehydration of cobalt formate dihydrate shown in Fig. 7 can be attributed to a phase-boundary controlled equation by comparing with the shape of the master curves in Fig. 8. In a phase-boundary controlled reaction of the R type, it has been considered that an interface is immediately formed at the edge and defect of a particle, and then advances into the center. This R-type reaction is characterized by the rapid initial production of a perfect reactant–product inter-

face at edges of the preferred crystallographic surface, and its rate depends on the advance of this interface [29]. Under these circumstances, all of this amounts to the surface of dehydrated particles being covered with minute amorphous products as observed in the XRD-DSC data, and the diffusion of the dissociated water molecules being retarded by the products. The amorphous products of the cobalt formate formed by process of dehydration will absorb the dissociated water molecules onto the narrow walls of their capillaries having molecular dimensions. This would interfere with the further escape of water molecules, and the rate of dehydration would, therefore, be slow.

Contrary to the case of the cobalt salt, however, the recrystallization of the anhydrous zinc formate formed by the dehydration occurs as indicated in the XRD-DSC data. As recrystallization is accompanied by the formation of wide channels among the dehydrated particles, through which the dissociated water molecules can easily escape, so the dehydration rate will become faster. In this case, it is satisfactory to consider that a rate-determining step of this dehydration mechanism is governed by the model of a nucleation and growth of the A type nuclei. Moreover, this interpretation is also in accordance with the CRTG analysis, because the experimental CDRC curve during dehydration of zinc formate dihydrate in Fig. 6 can be attributed to the reaction mechanism of an Avrami–Erofeev equation by comparing with the shape of the master curves in Fig. 8.

5. Conclusions

The CRTG have been used to analyze the complex thermal behavior in the dehydration of hydrated salts together with the new type of XRD-DSC. The XRD-DSC is especially powerful in collecting structural and thermal data on systems, where separate measurements under identical conditions are impractical, and in analyzing complicated dehydration behavior, because thermal changes (or overlapping changes) can be directly assigned to one or more structural events. The CRTG and the XRD-DSC are applied to zinc and cobalt formate dihydrates. The structural data obtained from the XRD-DSC gave the strongest proof of the kinetic equation of dehydration mechanisms obtained by CRTG (CDRC mode). These results clearly demonstrate the potential capability of these new experimental methods, XRD-DSC and CRTG, particularly for the examination of the complex phase-change behavior, inherent in many important reactions.

Acknowledgements

The authors would like to acknowledge Professor Yoshio Masuda of Niigata University, in providing guidelines for the scope, supplying the material and giving many pertinent comments.

References

[1] W.E. Brown, D. Dillimore, A.K. Gallway, in: C.H. Bamford, C.F.H. Tipper (Eds.), Comprehensive Chemical Kinetics, vol. 22, Reaction in the Solid State, Elsevier, Amsterdam, 1980, p. 1.
[2] B. Topley, M.L. Smith, J. Chem. Soc. 321 (1935).
[3] G. Thomas, J.J. Gardet, J.J. Gruffat, B. Guihot, M. Soustelle, J. Chim. Phys. 69 (1972) 375.
[4] T.A. Clarke, J.M. Thomas, J. Chem. Soc. Ser. A 2227 (1969) 2230.
[5] G. Bertrand, M. Lallemant, G. Watelle-Marion, J. Inorg. Nucl. Chem. 36 (1974) 1303.
[6] G. Bertrand, M. Lallemant, A. Mokhlisse, G. Watelle-Marion, J. Inorg. Nucl. Chem. 40 (1974) 819.
[7] T. Kimura, H. Imamura, M. Sugahara, T. Arii, S. Takagi, Mol. Cryst. Liq. Cryst. 276 (1996) 133.
[8] T. Arii, A. Kishi, Y. Kobayashi, submitted to Thermochim. Acta.
[9] J. Rouquerol, J. Therm. Anal. 2 (1970) 123.
[10] J. Rouquerol, Thermochim. Acta 144 (1989) 209.
[11] O.T. Sorensen, Thermochim. Acta 138 (1989) 107.
[12] F. Paulik, J. Paulik, Thermochim. Acta 100 (1986) 23.
[13] J.M. Criado, F.J. Gotor, A. Ortega, C. Real, Thermochim. Acta 199 (1992) 235.
[14] F. Rouquerol, J. Rouquerol, G. Thevand, M. Triaca, Surface Sic. 162 (1985) 239.
[15] J.M. Creado, F.J. Gotor, C. Real, F. Jimenez, S. Ramos, J. Del Cerro, Ferroelectrics 115 (1991) 43.
[16] S. Bordere, F. Rouquerol, J. Rouquerol, J. Esfienne, A. Floreancig, J. Therm. Anal. 36 (1990) 1651.
[17] T. Arii, T. Kanaya, A. Kishi, N. Fujii, Netsu Sokutei 21 (1994) 151.
[18] T. Arii, A. Kishi, N. Fujii, Netsu Sokutei 23 (1996) 5.
[19] T. Arii, T. Senda, N. Fujii, Thermochim. Acta 267 (1995) 209.
[20] T. Arii, K. Terayama, N. Fujii, J. Therm. Anal. 47 (1996) 1649.

[21] T. Arii, N. Fujii, J. Anal. Appl. Pyrolysis 39 (1997) 129.
[22] Y. Masuda, Netsu Sokutei 22 (1995) 203.
[23] Y. Masuda, K. Nagata, Thermochim. Acta 155 (1989) 255.
[24] T. Arii, H. Nakagawa, Y. Ichihara, N. Fujii, Thermochim. Acta, in press.
[25] T. Arii, J. Mass Spec. Soc. Jpn., in press.
[26] H. Tanaka, N. Koga, A.K. Galwey, J. Chem. Educ. 72 (1995) 251.
[27] H. Tanaka, Thermochim. Acta 267 (1995) 29.
[28] J.H. Sharp, G.W. Briendly, B.N.N. Acher, J. Am. Ceram., Soc. 49 (1966) 379.
[29] S.F. Hullbert, J. Br. Ceram. Soc. 6 (1969) 11.